Ocean–Atmosphere Interaction in the Making of the Walker Circulation and Equatorial Cold Tongue

SHANG-PING XIE

Graduate School of Environmental Earth Science, Hokkaido University, Sapporo, Japan

(Manuscript received 28 January 1997, in final form 12 May 1997)

ABSTRACT

The climate over the equatorial Pacific displays a pronounced asymmetry in the zonal direction that is characterized by the Walker circulation in the atmosphere and the cold tongue in the ocean. An intermediate coupled ocean–atmosphere model is used to investigate the driving force and the ocean–atmosphere interaction mechanism for the generation of the zonal asymmetry. In the far eastern Pacific, the upwelling at the equator is weak because zonal winds are blocked by the Andes. The off-equatorial upwelling induced by southerly cross-equatorial winds is thus crucial for cooling the eastern Pacific. A realistic cold tongue appears in the coupled model only when this southerly wind forcing is included. The southerly winds cause the sea surface temperature to fall in the east, enhancing the zonal heat contrast and hence intensifying easterly winds across the basin. These anomalous easterlies induce more equatorial upwelling and raise the thermocline in the east, amplifying the initial cooling by the southerlies. A simple analog model is presented to illustrate this coupled ocean–atmosphere feedback originally proposed by Bjerknes.

From an oceanographic point of view, the equatorial cold tongue is caused by easterly winds. In the coupled model, much of these easterlies arises as part of the Bjerknes feedback and can be attributed to the southerly wind forcing in the east. Were the earth climate symmetric about the equator, cross-equatorial wind would vanish, and the cold tongue would be much weaker and have a very different zonal structure than is observed today.

1. Introduction

The Pacific ocean–atmosphere system features large zonal variations along the equator (Fig. 1). A tongue of cold surface water extends from the coast of South America to the central Pacific, while the western Pacific records the highest sea surface temperatures (SSTs) in the World Ocean. On the atmospheric side, the rising branch of the so-called Walker circulation is located in the western Pacific and Indian Ocean sector as manifested by heavy rainfall, while the subsidence is observed in the eastern equatorial Pacific along with suppressed convective activity. From an oceanographic point of view, the cold tongue forms on the equator because of the easterly surface winds associated with the Walker circulation. From a meteorological point of view, on the other hand, the Walker circulation is maintained by the SST contrast between the east and west. The Walker circulation and the equatorial cold tongue are thus an interacting pair, each being both the cause and effect of the other. Bjerknes (1969) proposes an interaction mechanism for the development of this coupled pair. Suppose that the SST in the eastern Pacific cools a little for some reason. It will reduce the convective activity in the east, causing anomalous easterly winds. These easterly wind anomalies will enhance equatorial upwelling and raise the thermocline in the east, both of which lead to a further cooling of the surface ocean. As a mechanism for initiating the cooling in the east, Neelin and Dijkstra (1995) and Dijkstra and Neelin (1995) propose the easterly winds that are independent of zonal SST gradient and maintained by momentum transport by zonal mean circulation and midlatitude eddies.

In addition to the east–west asymmetries, the Pacific climatology also displays pronounced north–south asymmetries with respect to the equator. The intertropical convergence zone (ITCZ) stays in the Northern Hemisphere (NH) collocated with a zonal band of high sea surface temperature in the eastern Pacific (Fig. 1). Ocean–atmosphere interaction of different kinds operates to maintain such latitudinal asymmetries (Xie and Philander 1994; Philander et al. 1996). A coupled ocean–atmospheric wave, with a wind–evaporation–SST (WES) feedback as its restoring force, carries the signals of continental asymmetries far westward and establishes latitudinal asymmetries in both the ocean and atmosphere (Xie 1996; Ma et al. 1996; M. Kimoto and X. Shen 1995, personal communication). Southerly winds, which will become important for this study, blow

Corresponding author address: Prof. Shang-Ping Xie, Graduate School of Environmental Earth Science, Hokkaido University, Sapporo 060, Japan.
E-mail: xie@ee.hokudai.ac.jp

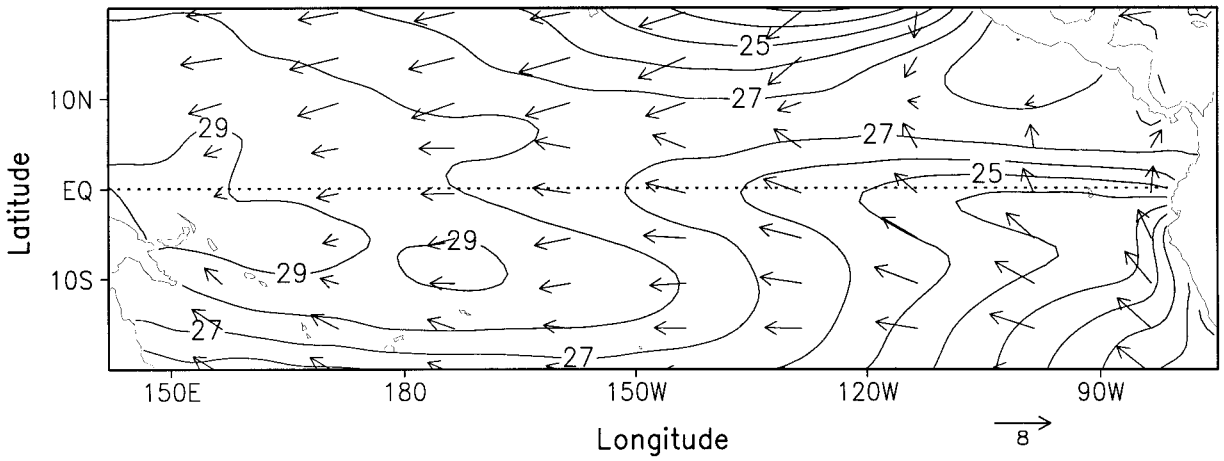

FIG. 1. Annual-mean sea surface temperature (contour) and surface wind vectors over the tropical Pacific.

across the equator over the eastern Pacific as a result of the establishment of latitudinal asymmetry.

The formation of zonal and latitudinal asymmetries over the Pacific is not two independent events. Large latitudinal asymmetries characterized by a single NH ITCZ develop only where the equatorial SST is low (Xie and Philander 1994). This paper proposes another connection between the two, with the NH ITCZ being a cause of the cold tongue this time. The equatorial cold tongue is generally considered an act of easterly winds through equatorial upwelling and rising thermocline. This conventional notion is not valid in the far eastern equatorial Pacific, where the zonal wind vanishes presumably due to the blocking of the Andes (Fig. 1). Without the upwelling pumping up the cold subsurface water, sea surface temperature in the eastern Pacific would be as high as in the warm pool despite shallow thermocline. The cross-equatorial southerly winds are the cause of cold sea surface temperature in the far eastern Pacific. Figure 2 shows a meridional section of ocean temperature along 90°W. The thermocline rises to the south while it deepens to the north of the equator, characteristic of the oceanic response to cross-equatorial southerly winds and indicative of upwelling (downwelling) south (north) of the equator (Philander and Pacanowski 1981). As a manifestation of the southern upwelling, the SST minimum is found slightly south of the equator. The center of the cold tongue consistently shifts to the south of the equator in the eastern Pacific (Fig. 1), moving back to the equator only in the central Pacific as easterly winds intensify and equatorial upwelling takes over. In addition to the southern upwelling in the open ocean, the southerly winds also cause upwelling along the west coast of South America, helping to cool the equatorial eastern Pacific. Were the Pacific symmetric about the equator, meridional winds would vanish at the equator. Neither southern upwelling nor equatorward advection of cold coastal water would be possible. As a result, the SST in the eastern Pacific would be much warmer (see the next section and Fig. 4). From an oceanographic point of view the effect of southerly winds may seem to be limited to the eastern Pacific, but because of ocean–atmosphere feedbacks, their real effect on the coupled system needs to be investigated.

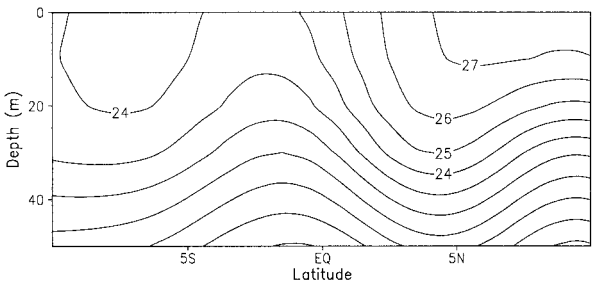

FIG. 2. Latitude–depth section of ocean temperature along 90°W in the eastern Pacific.

The above association of zonal asymmetry with cross-equatorial wind is also seen in the seasonal advance and retreat of the equatorial cold tongue. In response to the seasonal march of the sun, the southerly winds intensify in boreal summer but relax in boreal winter. This annual cycle in meridional wind forces an annual cycle in SST in the eastern Pacific (Fig. 3), where the thermocline is shallow and the annual-mean winds are southerly (Mitchell and Wallace 1992; Xie 1994). The SST annual cycle induces an annual cycle in the zonal wind, which in turn modifies SST. This Bjerknes feedback produces the coherent westward propagation of annual signals in SST and zonal wind.

The present study investigates the role of southerly cross-equatorial winds in the coupled development of the Walker circulation and cold tongue. We will focus on an equatorial region, say, within 5° of the equator, where upwelling/downwelling is the dominant mechanism for SST changes. Features produced by processes outside will be specified as external forcing. A stripped-down version of the Zebiak and Cane (1987) model is

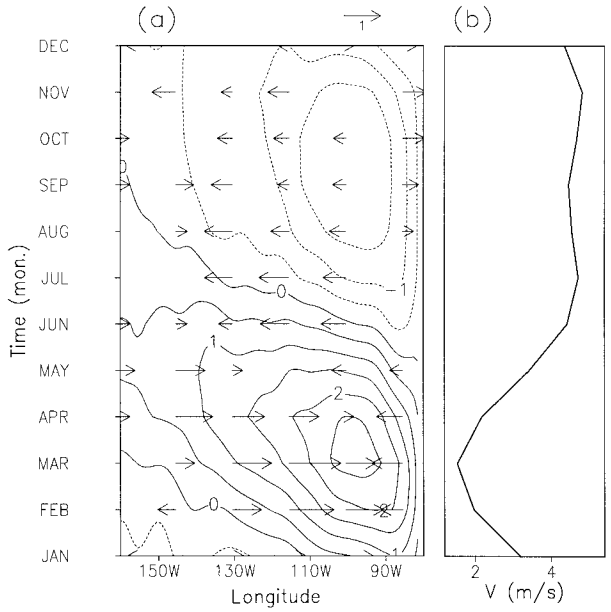

FIG. 3. Equatorial annual cycle. (a) Time–longitude section of departures of sea surface temperature (contour) and surface zonal wind velocity (vector) from their annual means. (b) Cross-equatorial southerly wind velocity averaged between 110° and 80°W as a function of time.

modified to include not only the equatorial upwelling induced by zonal wind but the southern upwelling by meridional wind as well. This model calculates SST along the center line of the cold tongue and contains the minimum physics necessary for describing zonal asymmetry. We will examine how the southerly wind forcing affects the intensity and zonal structure of the cold tongue. As we will see, the model produces a realistic cold tongue only when southerly wind forcing is included. The Bjerknes feedback acts not only to amplify the cooling in the east, but also to expand the cold tongue toward the west. A simple conceptual model is developed to illustrate the working of the Bjerknes feedback in the presence of southerly wind forcing.

The next section describes the model and its simulation of zonal SST distribution when it is forced with observed winds. Section 3 presents results from the coupled model, while section 4 derives the simple model. Section 5 is the summary.

2. Model

An intermediate coupled ocean–atmosphere model based on Jin and Neelin (1993) and Dijkstra and Neelin (1995) is used. It couples a stripped-down version of the Zebiak and Cane (1987) ocean model with the Matsuno (1966) and Gill (1980) atmosphere.

a. Ocean model

The ocean model computes the sea surface temperature (T) along the center line of the equatorial cold tongue where $\partial T/\partial y = 0$ by definition so that the governing equation for T becomes

$$T_t = -H(w)w(T - T_e)/H_{1.5} - \varepsilon_T(T - T_0). \quad (2.1)$$

Advection by the westward South Equatorial Current pushes the cold tongue a little westward. Other than this, experiments with and without the zonal advection give the same results. The zonal advection term is thus neglected to keep the model simple (Hao et al. 1993; Neelin and Dijkstra 1995). In (2.1), $H(w)$ is the Heaviside function, w is the vertical velocity at $H_1 = 50$ m, and ε_T is the coefficient for the thermal damping due to surface heat flux. The equilibrium temperature T_0 is given as a spatial constant, although it is a function of cloudiness, wind speed, and other variables in reality. Subsurface temperature T_e at $H_{1.5} = 2H_1 = 100$ m is parameterized as a function of thermocline depth h:

$$T_e = T_0 - \frac{\Delta T}{2}\left[1 + \tanh\left(\frac{h + h_0}{H^*}\right)\right]. \quad (2.2)$$

The thermocline depth at the equator, h_e, is obtained by solving a reduced gravity model forcing a zonal wind distribution $\tau_x(x)$:

$$h_e(x) = \frac{L}{g'}\left[\int_0^1 s^{1/2}\tau_x(s)\,ds - \int_x^1 \tau_x(s)\,ds\right]. \quad (2.3)$$

Here it is assumed that the meridional scale of the wind pattern is large enough and that the mechanic damping timescale is much longer than the time for the Kelvin wave to cross the basin (Hao et al. 1993; Cane et al. 1990). In (2.3), L is the basin size, g' is the reduced gravity parameter, and $\tau_x = \tau_x^*|_{y=0}/(\rho H)$, with τ_x^* being the zonal wind stress in N m^{-2}, ρ the water density, and H the mean thermocline depth.

The upwelling velocity is calculated from the divergence of the current shear between the frictional surface layer and the rest of the thermocline. Both zonal and meridional winds can cause upwelling near the equator. In response to a spatially uniform wind of both components the largest upwelling occurs off the equator at

$$y = y_w \equiv \alpha\varepsilon/\beta, \quad (2.4)$$

where ε is the interfacial damping rate for momentum, β is the meridional gradient of the Coriolis parameter, and

$$\alpha = -\tau_x/\tau_y - \text{sign}(\tau_y)[1 + (\tau_x/\tau_y)^2]^{1/2}.$$

In particular, $\alpha = 0$ for $\tau_y = 0$, and $\alpha = -1$ for $\tau_x = 0$ and $\tau_y > 0$. The maximum upwelling velocity is

$$w = -b_w[(1 - \alpha^2)\tau_x + 2\alpha\tau_y]/(1 + \alpha^2)^2, \quad (2.5)$$

where $b_w = H_2\beta/\varepsilon^2$ with $H_2 = H - H_1$. The effect of spatial variations in wind stress will not be considered, given that the meridional scale of wind stress field is of the order of the atmospheric radius of deformation, much larger than either the oceanic radius of deformation or the frictional length scale ε/β. In the absence

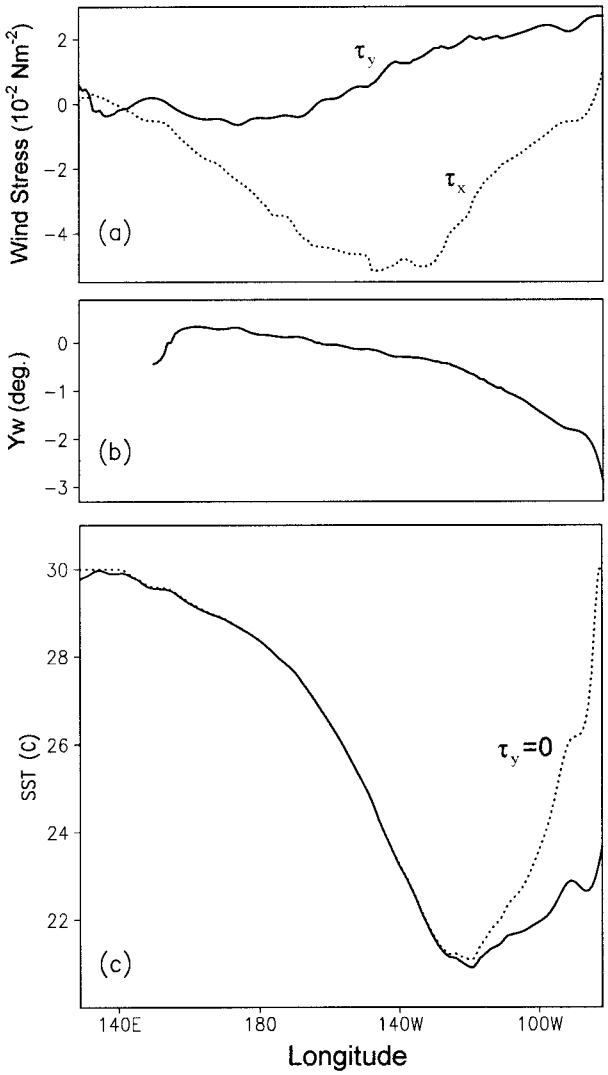

FIG. 4. Zonal distributions of (a) observed wind stresses on the equator, (b) latitude of maximum upwelling, and (c) sea surface temperature at the latitude of maximum upwelling as simulated in the ocean model with (solid) and without (dotted) southerly wind forcing.

of zonal advection, the latitude of the maximum upwelling coincides with that of the SST minimum so that (2.5) will be used to compute the entrainment rate. In the eastern Pacific, the difference in h between the equator and the latitude of maximum upwelling is small compared to its change in the zonal direction, both because zonal wind is much more efficient in displacing the thermocline than meridional wind and because the thermocline response to a zonal wind forcing has a large meridional scale toward the east. Therefore we let

$$h(y = y_w) = h_e. \tag{2.6}$$

To test the model's ability to simulate the climatology of the Pacific, we force the model with observed annual-mean COADS (Comprehensive Ocean–Atmosphere Data Set; Woodruff et al. 1987) wind stresses that are averaged within 3° of the equator (Fig. 4a). The model parameters (Table 1) have the same values as in Hao et al. (1993). Figure 4c displays the simulated SST distribution along the center line of the cold tongue. As pointed out in the introduction, the easterly winds over the eastern Pacific are too weak to cool the ocean surface (dotted line). The cross-equatorial southerly winds induce upwelling to the south of the equator (Fig. 4b), which is crucial to maintaining the cold sea surface temperatures in the east (solid line of Fig. 4c). When forced by both components of wind, the model is able to simulate the gross features of the SST distribution, with an east–west SST difference of 9°. This gives us some confidence in the usefulness of the model and in our selection of parameter values. Compared to observations, the region of the coldest temperature is too far westward off the coast, presumably because the model neglects cloud forcing and advection of coastal water. Huang and Schneider (1995) discussed how changes in the alongshore southerly winds on the South American coast affect the SSTs in the far eastern Pacific. In this stand-alone ocean model simulation, the effect of meridional wind is limited to the eastern basin because toward the west, the southerly wind weakens and the thermocline deepens. When the ocean and atmosphere are allowed to fully interact, the effect of the southerly forcing may not be trapped by the coast.

TABLE 1. Model parameters.

Variable	Value
$\rho H\bar{\tau}_x$	-0.01 N m^{-2}
$\rho H\tau_0$	0.015 N m^{-2}
A	0.025 N m^{-2} K^{-1}
ε_a	2.5
ε_T^{-1}	180 days
ε^{-1}	2 days
g'	0.02 m s^{-2}
h_0	30 m
H^*	50 m
H	200 m
H_1	50 m
T_0	30°C
T_c	29°C
ΔT	16°C
L	1.65×10^7 m

b. Atmosphere model

In response to an equatorial heat source that is evanescent poleward in the form of a Gaussian function with a half-width of the atmospheric deformation radius, the Matsuno–Gill model under the longwave approximation gives the distribution of zonal wind at the equator:

$$U' = \frac{\varepsilon_a}{2}\left[3e^{3\varepsilon_a x}\int_x^1 Q'(s)e^{-3\varepsilon_a s}\,ds - e^{-\varepsilon_a x}\int_0^x Q'(s)e^{\varepsilon_a s}\,ds\right], \quad (2.7)$$

where $Q'(x)$ is the zonal distribution of the heating at the equator, x is the zonal coordinate nondimensionalized with L, and ε_a is the atmospheric damping rate nondimensionalized with C/L (C: the phase speed of the atmospheric Kelvin wave). Here only the Pacific is allowed to change its surface temperature and the associated heating anomalies are assumed to be proportional to the SST's departure from a reference temperature, T_c,

$$Q' = K(T - T_c). \quad (2.8)$$

Heating anomalies outside the Pacific domain are set to zero. The value of T_c is chosen to be slightly smaller than T_0 because background vertical mixing will keep the SST in the western Pacific below T_0, the equilibrium temperature imposed by surface heat flux. In practice, the coupled model results are not sensitive to the choice of T_c within a range of 1°C.

Generally, SST has meridional structures more complicated than the Gaussian function, exciting more than just the Kelvin and first Rossby waves. Hao et al. (1993) interpret (2.7) as a truncated version of the full Matsuno–Gill model and report that higher-order truncations give, qualitatively, the same results.

Even in the absence of any zonal variation in SST, easterly winds would still be present at the equator because of the momentum transport by eddies and by zonal mean Hadley circulation. In fact, equatorial winds are easterly in zonally symmetric aquaplanet GCMs (Numaguti and Hayashi 1992). This zonal mean easterly is one of the forces that drives the Pacific climate away from zonal symmetry. Thus the total zonal wind at the equator is the sum of U' and the external easterly $\overline{U}$,

$$U = \overline{U} + U'. \quad (2.9)$$

The above is the formulation of the atmospheric model for nearly all intermediate coupled models, including the one used by Neelin and Dijkstra (1995). It neglects the effect of the Andean Mountains. It is not a problem for studies of El Niño–Southern Oscillation (ENSO) since the ENSO-related convective heating anomalies are centered on the central Pacific, causing little change in the zonal wind over the eastern Pacific.

However, the Andes have a pronounced effect on the distribution of the mean zonal wind along the equator, blocking the flow in the lower troposphere. Here, a condition of nonnormal flow is imposed on the eastern boundary of the Pacific:

$$U|_{x=0} = 0. \quad (2.10)$$

This boundary condition is proper if the model is interpreted as the one for the planetary boundary layer (Lindzen and Nigam 1987). The use of (2.10) would be hard to formally justify if the model represents the first baroclinic mode of the troposphere. But intuitively, (2.10) should give a right sense of the Andes blocking effect on surface flow. In a two-level model, the low-level wind distribution below the mountains resembles that with the Andes as a full barrier that blocks the whole troposphere (Kleeman 1989). Boundary condition (2.10) should be viewed as a crude representation of the Andes effect on the surface flow, and a better treatment of the mountains is needed in future studies.

To be consistent with the truncation in (2.7), we will include only the first equatorial Rossby mode reflected on the eastern boundary to satisfy the boundary condition (2.10), though it is easy to include higher-order Rossby modes as well. As a result, the zonal wind at the equator is given by

$$U = \overline{U} + U' - (\overline{U} + U')|_{x=0}e^{-3\varepsilon_a(1-x)}. \quad (2.11)$$

The third term on the rhs represents winds associated with the reflected Rossby wave.

c. Coupling

A linear drag law is used to compute wind stress, which with the help of (2.7) becomes

$$\rho H\tau_x' = A\frac{\varepsilon_a}{2}\left[3e^{3\varepsilon_a x}\int_x^1 T'(s)e^{-3\varepsilon_a s}\,ds - e^{-\varepsilon_a x}\int_0^x T'(s)e^{\varepsilon_a s}\,ds\right], \quad (2.12)$$

where $A = K\rho_a C_D U_O$ with C_D being the drag coefficient and U_0 a characteristic scalar wind speed, and $T' = T - T_c$. The zonal wind stress affects sea surface temperature in two ways: by changing the entrainment temperature [see (2.2) and (2.3)] and by inducing upwelling [see (2.5)].

The presence of southerly cross-equatorial winds in the eastern Pacific enhances the upwelling and thus the entrainment of the cold thermocline water. The change in the southerly wind affects upwelling velocity in a nonlinear way as can be seen in (2.5). For the purpose of a qualitative demonstration of the southerly wind effect, we may neglect this nonlinearity and let the total upwelling be the sum of upwelling induced separately by easterly and southerly stresses:

$$w = b_w(-\tau_x + |\tau_y|/2), \quad (2.13)$$

where the first and second terms in the parentheses are obtained by letting $\alpha = 0$ and $\alpha = -1$ in (2.5), respectively. In this study, the southerly winds on the equator are imposed in a simple functional form:

$$\tau_y = (\tau_0/2)\{1 + \tanh[(x - x_0)/\Delta x]\}, \quad (2.14)$$

with $x_0 = -0.2$ and $\Delta x = 0.1$. The southerly stress decays rapidly away from the eastern boundary, reduc-

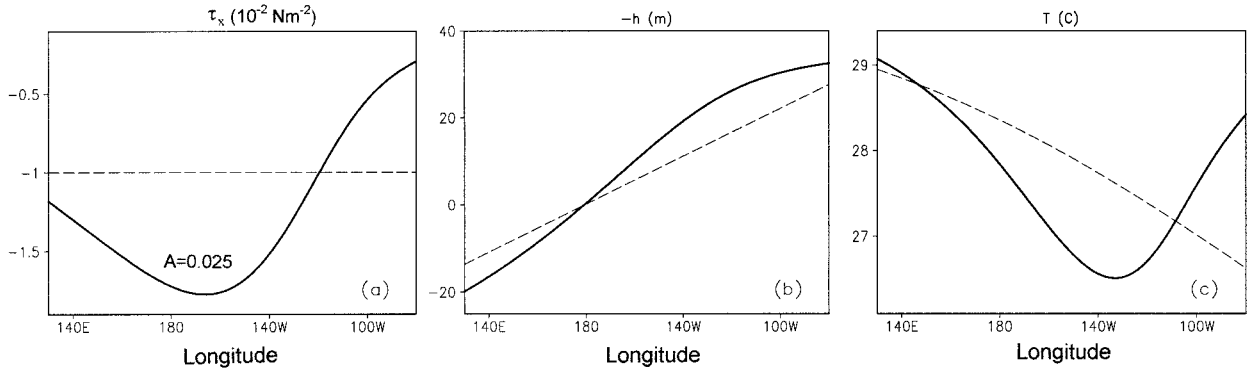

FIG. 5. Coupled (solid) and uncoupled (dashed) model solutions without southerly wind forcing: (a) zonal wind stress, (b) thermocline depth, and (c) sea surface temperature along the equator.

ing to one-half 30° longitude off the coast and to less than a quarter 15° farther to the west. In the equatorial eastern Pacific where the winds remain southerly throughout the year, the seasonal cycle has no direct effect on the annual-mean upwelling velocity. In a hypothetical climate that is symmetric about the equator, the cross-equatorial wind would swing between southerly and northerly, leaving a nonzero annual-mean upwelling cooling.

The prescribed easterly $\overline{U}$ and southerly τ_y are the two external forces that drive the equatorial atmosphere–ocean system away from zonal symmetry. While both contribute to upwelling cold water from the thermocline, $\overline{U}$ has the further effect of raising the thermocline in the east. When the coupling is activated between the ocean and atmosphere, the zonal wind changes both in strength and spatial structure as part of the Bjerknes feedback while the southerly remains unchanged and confined to the eastern ocean. In the following experiments, these external easterly and southerly winds are prescribed of modest magnitudes with $\rho H\overline{\tau}_x = -0.01$ N m^{-2} and $\rho H\tau_y = 0.015$ N m^{-2}. The model equations are solved by finite differences in both time and space in a domain of the Pacific size ($L =$ 16 500 km), with a spatial resolution of 110 km.

3. Results

This section presents results from two model runs, one with and one without the southerly forcing. The effects of the southerly winds will be illustrated by comparing results from these two experiments.

a. The $\tau_y = 0$ case

We first run the model under a conventional setting with $\tau_y = 0$ and the Andes removed. Figure 5 depicts the zonal wind, thermocline depth, and sea surface temperature along the equator with the uncoupled solution shown in dashed lines. Without any feedback from the atmosphere, a tilt of the thermocline is set up by the imposed easterly wind with shallow depth in the east. External easterly $\overline{\tau}_x$ induces a zonally uniform upwelling along the equator, cooling the east more than the west because the upwelled water has lower temperatures in the east. The SST in the west remains high and is close to T_c. Upon activating ocean–atmosphere coupling (solid lines), the zonal SST contrast within the model Pacific enhances the easterly winds in the western two-thirds of the basin. Consequently, the SST decreases where the easterlies are enhanced. In the eastern Pacific, however, the heat contrast between the cold ocean and warm land induces westerly wind anomalies, weakening the equatorial upwelling. Because the relaxed winds nearly offset the intensified easterlies in the western two-thirds of the basin, the rise of the thermocline is modest in the east, not enough to overcome the warming due to the reduced upwelling. The SST in the east increases as a result.

The right panel of Fig. 6 shows how the zonal SST distribution evolves as the coupling strengthens. No matter how strong the coupling between the ocean and atmosphere is, the cold tongue does not intensify and the minimum SST along the equator remains almost unchanged. The Bjerknes feedback operates here to move the region of the minimum SST westward by reducing SST in the central ocean while raising the temperature in the east. This is consistent with existing theories of equatorial ocean–atmosphere interaction; surface processes associated with upwelling tend to move coupled disturbances westward while the thermocline depth feedback favors an eastward propagation (Hirst 1986; Neelin 1991; Jin et al. 1993). Obviously upwelling feedback is dominant here.

This difficulty in producing a realistic SST distribution can be avoided by reducing the contribution of perturbation upwelling. Dijkstra and Neelin (1995) partition the upwelling into two parts, the one caused by the external easterly and the one by internally generated winds. Different rates of efficiency in inducing upwelling, δ_F and δ_s with $\delta_F \gg \delta_s$, are assigned to external and internal winds, respectively:

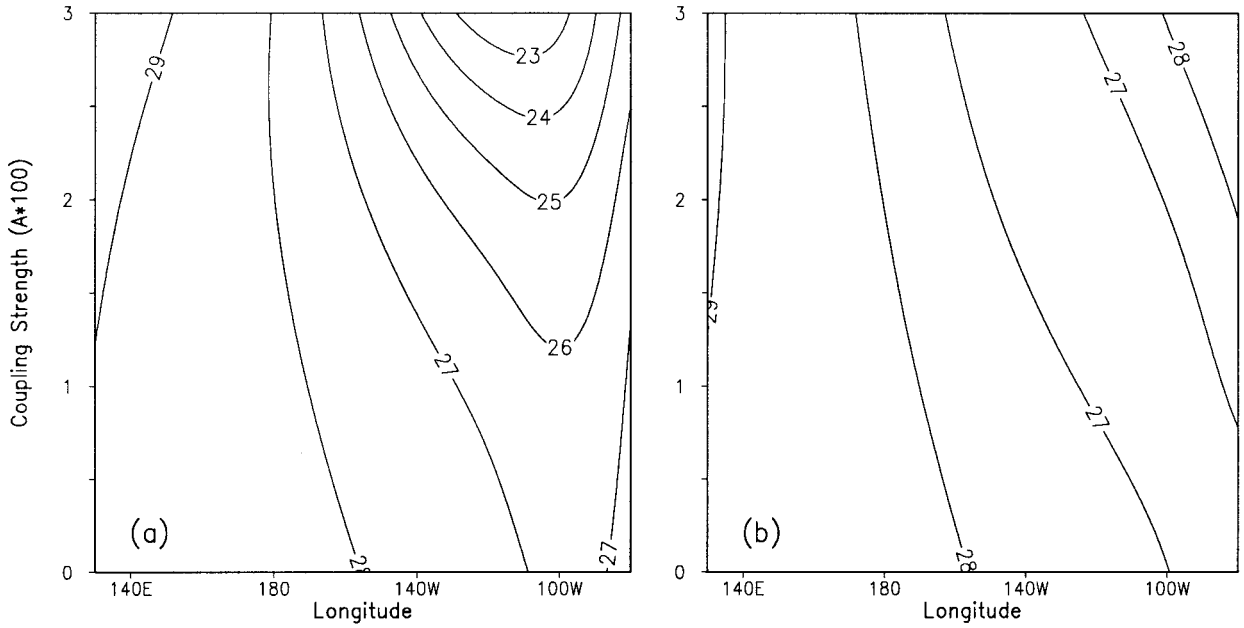

FIG. 6. Zonal distribution of sea surface temperature in model runs (left) with and (right) without southerly wind forcing along the maximum upwelling line as a function of coupling strength.

$$w \propto -(\delta_F \overline{\tau}_x + \delta_s \tau'_x)$$

[see their (A3)]. By varying δ_s as a control parameter, they are able to demonstrate that upwelling and thermocline displacement play different roles in shaping the zonal SST distribution. Physically, however, the external and internal winds should induce upwelling with the same efficiency, and δ_F and δ_s should be equal. Additional experiments (not shown) indicate that the use of small values of δ_s/δ_F, which tends to emphasize the thermocline depth feedback, is the cause of the difference of their results from the present $\tau_y = 0$ experiment.

b. *Effects of southerly winds*

We now switch on the southerly winds and add the mountains so that the zonal wind vanishes on the eastern boundary of the ocean. Drastic differences emerge in the development of the cold tongue. The cold tongue intensifies with the increase of coupling strength (Fig. 6a). The region of the lowest SST is anchored to the east while the cold tongue expands toward the west. The southerly winds play the role of anchor, keeping the eastern ocean cool by upwelling cold thermocline water.

Figure 7 depicts the zonal structures of the coupled model solution. The easterly winds intensify throughout the basin with the strongest easterly now occurring in the middle of the ocean basin, resembling the observed wind distribution. This enhancement in the easterly wind stress is balanced by an increased tilt of the thermocline. A shallow thermocline coupled with strong upwelling causes sea surface temperature to decrease in the eastern two-thirds of the basin. Of course, the intensification of easterly winds itself arises as a result of this cooling of the eastern ocean in the first place. This

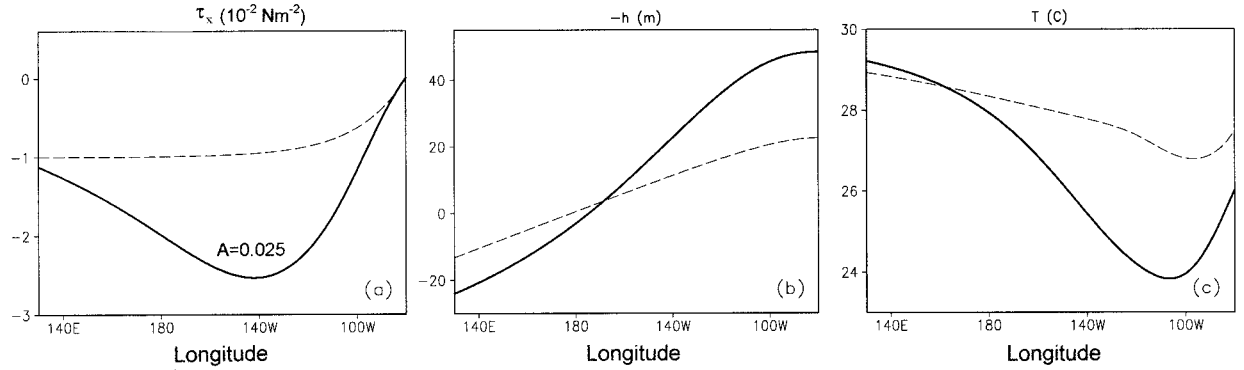

FIG. 7. Same as Fig. 5 except for the runs with the southerly wind forcing.

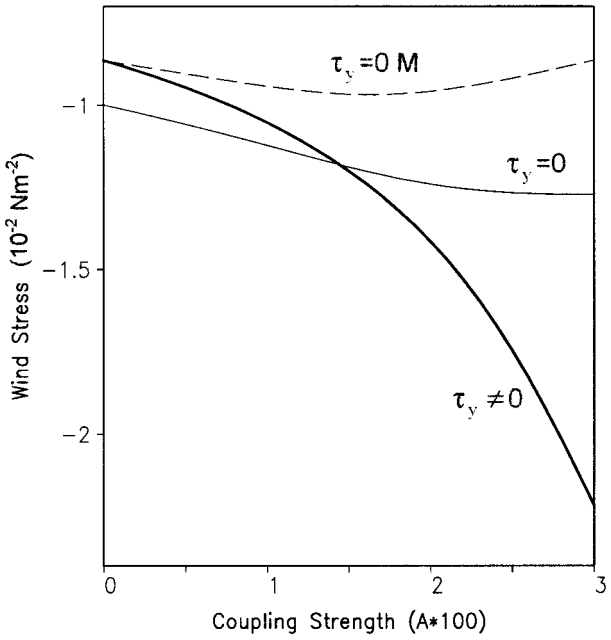

FIG. 8. Basin-wide average of zonal wind stress as a function of coupling strength.

is the familiar Bjerknes feedback mechanism that is central to the development of the cold tongue in the model. The direct cooling effect of the southerly winds on the SST is limited to a small region in the east, as in the stand-alone ocean model simulation (Fig. 4). Thanks to the Bjerknes feedback, the response of the coupled ocean–atmosphere system to this southerly forcing is much more pronounced and reaches the whole Pacific Ocean basin. Much of the enhanced easterlies that are crucial for maintaining the cold tongue can be attributed to the seemingly local effect of the southerlies. This is an example that a forced ocean model simulation may not reveal the real causality.

Figure 8 shows the zonal wind speed averaged across the basin as a function of coupling strength, which determines the thermocline depth difference between the eastern and western boundaries and may serve as a global measure of zonal asymmetry. In the $\tau_y = 0$ case, the Bjerknes feedback acts not to enhance the zonal asymmetry but rather to change its zonal structure. As a result, the basin mean easterly speed increases only slightly with the coupling coefficient. In contrast, the zonal asymmetry intensifies rapidly as coupling strengthens in the $\tau_y \neq 0$ case. The rate of increase is not linear, being greater at stronger coupling. We will return to this point later.

The role of the southerly winds and the working of the Bjerknes feedback can be seen from a different perspective of initial value problems. Initially, the SST is set to be uniformly 30°C along the equator and then the external winds suddenly act upon the ocean. Figure 9 shows the time–longitude evolution of the coupled system afterward. In the first three months, the response is quite similar between the $\tau_y \neq 0$ and $\tau_y = 0$ cases. The SST starts to fall everywhere in the basin, with the largest cooling taking place in the east. Then the Bjerknes feedback kicks in, operating very differently with and without southerly wind forcing. It keeps cooling the eastern ocean with the help of southerlies but pushes the cold water away toward the west in the $\tau_y = 0$ case. The $\tau_y \neq 0$ case seems to take a longer time to reach the steady state. It is interesting to note that the time–longitude sections are similar to Fig. 6 with the time coordinate replaced by the coupling coefficient.

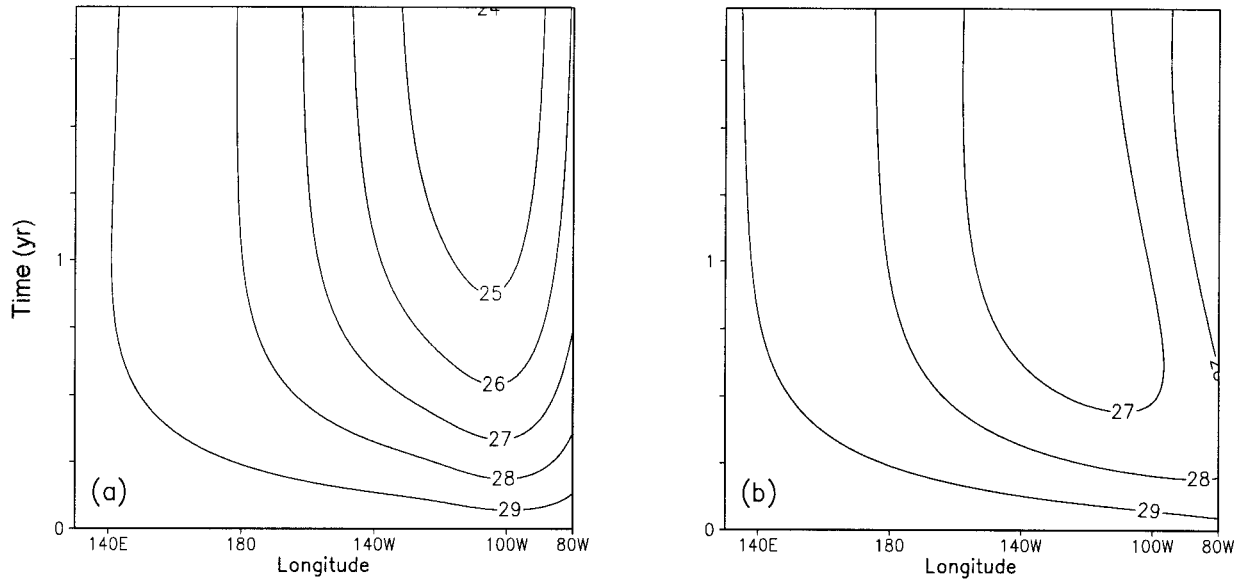

FIG. 9. Time–longitude section of sea surface temperature (left) with and (right) without the southerly wind forcing. The initial field of sea surface temperature is zonally uniform.

4. A simple model

Simple analytical coupled models, pioneered by Suarez and Schopf (1988) and Battisti and Hirst (1989), prove to be a useful tool for understanding the interaction of the ocean and atmosphere. Neelin and Dijkstra (1995) present such a simple ''toy'' model for the problem of climatological zonal asymmetry. All of these simple models are so-called point-coupling models, concerning only the average temperature in the eastern Pacific while assuming temperature elsewhere invariant. As such, this type of model does not resolve the zonal structure of the disturbance. As seen in the last section, the Bjerknes feedback acts not only to strengthen the zonal asymmetry, but to change its zonal structure as well. Here we extend the work of Neelin and Dijkstra by retaining the zonal dimension in the model. As a cautionary note, these models are useful only for describing qualitative features of the full model as their derivation relies heavily on physical intuitions rather than formal justification.

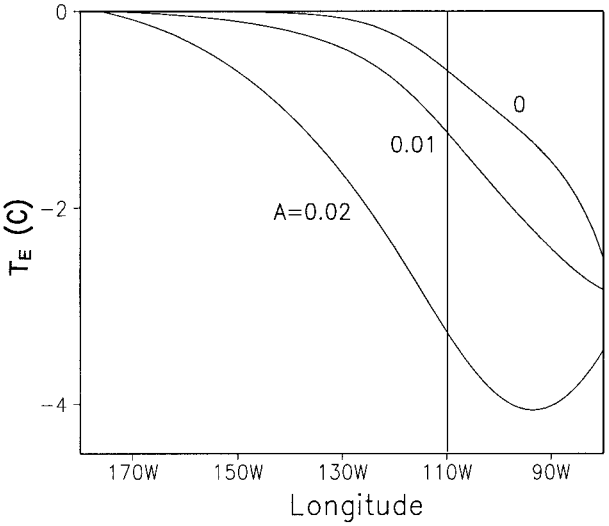

FIG. 10. Sea surface temperature anomaly forced by southerly winds as a function of longitude.

a. Model equations

We will focus on the coupled ocean–atmospheric response to southerly wind forcing. For this purpose, we choose a basic state that is the solution for the model run with $\tau_y = 0$ but with the mountain blockage included. We will call this the $\tau_y = 0$ M case to distinguish it from the $\tau_y = 0$ case presented in section 3a. The basin mean easterly wind speed for the $\tau_y = 0$ M case shows little dependence on coupling strength (dashed line in Fig. 8). Overall, the solution for the $\tau_y = 0$ M case looks similar to that for the $\tau_y = 0$ case, with the SST minimum located in the central Pacific. The SST at the eastern boundary is high and equal to the equilibrium temperature T_0 because of the vanishing zonal wind. Notation in this section is such that the overbar denotes basic-state variables while the prime shows departures (anomalies) from this basic state. Figure 10 shows southerly forced SST anomalies, which are largest in the east.

Anomalous upwelling is caused by anomalous zonal wind from (2.13):

$$w' = -b\tau', \tag{4.1}$$

where $b = b_w/H_{1.5}$. The zonal wind stress is balanced by the thermocline tilt; taking the derivative of (2.3) with respect to x yields

$$-g'\frac{\partial h'}{\partial x} + \tau' = 0. \tag{4.2}$$

Note that x *is* redimensionalized in this section. The variables are decomposed into mean and anomaly

$$w = \overline{w} + w_y + w', \tag{4.3a}$$

$$T = \overline{T} + T', \quad \text{and} \tag{4.3b}$$

$$T_e = \overline{T}_e + \alpha h', \tag{4.3c}$$

where $w_y = b\tau_y/2$ is the southerly wind-induced upwelling and $\alpha = \partial T_e/\partial h$. Here we consider a case of weak southerly wind forcing, $\xi = w_y/\overline{w} < 1$. Substituting (4.3) in (2.1) and retaining $o(\xi)$ terms, we obtain a linear equation for T':

$$\overline{w}\alpha h' - w'(\overline{T} - \overline{T}_e) - ET' - w_y(\overline{T} - \overline{T}_e) = 0, \tag{4.4}$$

where $E = \varepsilon_T + \overline{w}$. Note that $o(w') = o(w_y)$. Similar linearization is possible for a case of finite w_y but small coupling coefficient. The first term on the lhs of (4.4) is the warming associated with the deepening of thermocline, the second is the cooling caused by the upwelling anomaly, and the fourth is the upwelling cooling by the southerly winds and appears as an external forcing.

A simple linear proportional relation seems to exist between SST gradient and zonal wind-stress anomalies:

$$\tau' = \mu\frac{\partial T'}{\partial x}, \tag{4.5}$$

where μ is the coupling coefficient. This simple relation is confirmed by the scatterplot based on the $\tau_y \neq 0$ runs with various coupling coefficients (Fig. 11). Equation (4.5) is proposed by Lindzen and Nigam (1987) as an alternative of the Matsuno–Gill model. Within the decay length scale of the reflected Rossby wave [$1/(3\varepsilon_a) \sim$ 2000 km] off the eastern boundary, the situation is more complicated and (4.5) is not valid. Equations (4.1)–(4.2) and (4.4)–(4.5) form a complete set, which will be solved in the eastern and interior regions separately.

b. Interior solution

Because the southerly winds are confined to a small region in the east, the interior ocean is not under their direct forcing so

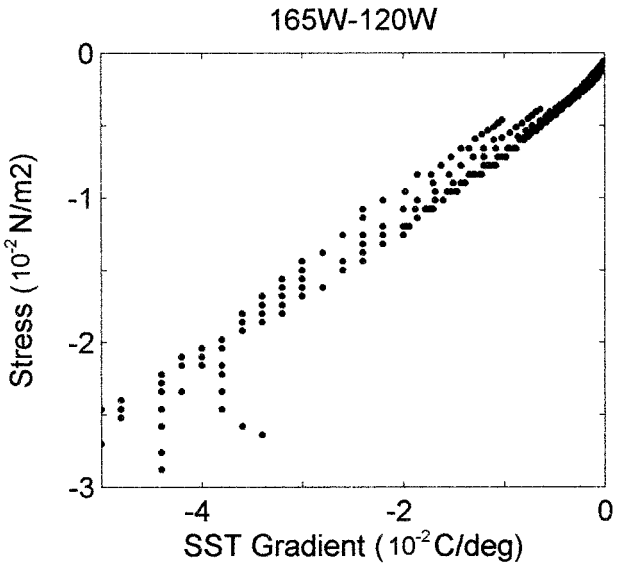

FIG. 11. Scatterplot of zonal wind stress and sea surface temperature gradient in the central part of the model Pacific. Wind stress is scaled with the coupling coefficient $\tilde{\tau}_x = A_0\tau_x/A$ with $A_0 = 0.03$ N m^{-2}.

$$w_y \approx 0. \tag{4.6}$$

We will further ignore the effect of thermocline depth change because the mean thermocline is relatively deep and h′ is largest at the eastern boundary. Thus,

$$\alpha h' \approx 0. \tag{4.7}$$

With the help of (4.6) and (4.7), the SST equation (4.4) is simplified

$$\mu(\overline{T} - \overline{T}_e)\frac{\partial T'}{\partial x} + ET' = 0, \tag{4.8}$$

which is solved under the boundary condition

$$T'|_{x=x_E} = T_E, \tag{4.9}$$

where the SST in the east, T_E, will be determined later. The formal solution to (4.8) and (4.9) is then

$$T' = T_E e^{(x-x_E)/a}, \tag{4.10}$$

where

$$a = \mu(\overline{T} - \overline{T}_e)/E \tag{4.11}$$

determines how far the SST anomaly forced in the east can extend into the west. Here we neglect zonal variations of the basic state in this interior region for simplicity, but the solution for a spatially varying basic state can be readily obtained.

c. Forced solution in the east

We now consider the coupled response in the eastern region $x_E < x < 0$ that is under the direct forcing of the southerly winds. The rate of upwelling induced by zonal wind anomaly at $x = x_E$ can be obtained by substituting (4.10) in (4.5) and (4.1):

$$w_E = -\frac{\mu b}{a}T_E, \tag{4.12}$$

where the subscript E denotes anomaly in the east. By assuming both SST and thermocline depth anomalies are negligible in the far west, integrating (4.2) leads to

$$h_E = \mu T_E/g'. \tag{4.13}$$

With $w'|_{x=0} = 0$, an estimate of the upwelling rate averaged within $x_E < x < 0$ is $[w'] = w_E/2$, where the bracket denotes the area average. As a crude estimate of other area averages, we let $[h'] = h_E$ and $[T'] = T_E$. Then a solution to (4.4) is

$$T_E = -\frac{w_y(\overline{T} - \overline{T}_e)}{E - \mu F}, \tag{4.14}$$

where

$$F = \frac{\alpha\overline{w}}{g'} + \frac{b(\overline{T} - \overline{T}_e)}{2a} > 0. \tag{4.15}$$

Equations (4.12) and (4.13) are common assumptions for other point-coupling models, and in fact, (4.14) is the same as the linearized toy model of Neelin and Dijkstra (1995) except that w_y is replaced with $(-b\overline{\tau}_x)$ in their analysis.

Equation (4.14) gives the SST response to southerly wind forcing in the east. The magnitude of the response depends on the size of the thermal resistance $(E - \mu F)$ that decreases as coupling intensifies. The Bjerknes feedback thus acts to enhance the temperature response in the east, but its effect is not limited to the region that is under the direct forcing of the southerly winds. It spreads the forcing effect far westward into the central Pacific where SST changes would otherwise be zero. Equation (4.11) states that the *e*-folding scale of the westward expansion of the coupled response is proportional to the coupling strength. By treating the coupled system separately in the forced and unforced regions, the two separate roles of the Bjerknes feedback—as an amplifier and as a signal transmitter—become clear.

At high coupling, the denominator on the rhs of (4.14) becomes negative and this linear theory is no longer valid. This corresponds to an unstable regime where zonal asymmetry develops spontaneously without any external forcing (Neelin and Dijkstra 1995; Liu and Huang 1997). Thus the degree of asymmetry the model finally reaches and its zonal structures are less dependent on the external forcing than on the nonlinearity and structures of the dominant unstable modes. Since the present intermediate model is obviously in a stable regime, the model behavior in the unstable regime will not be further discussed.

We now reanalyze the intermediate model results in light of the above theory. The western edge of the forced region is chosen to be 30° west of the eastern boundary

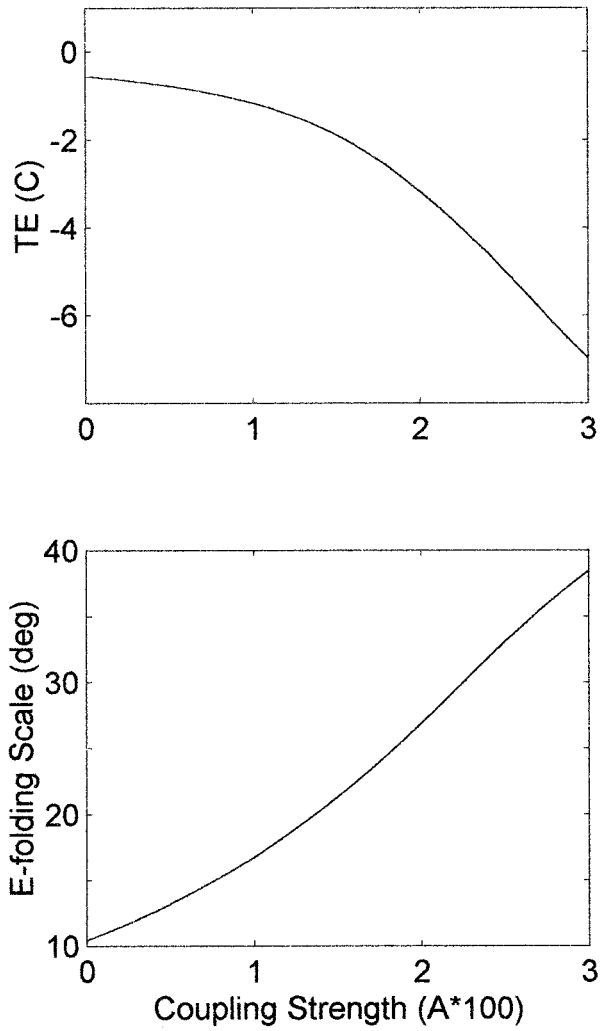

FIG. 12. Southerly wind-forced sea surface temperature anomaly at 110°W (T_E; upper), and *e*-folding length scale for its westward decay (lower) as a function of coupling strength (10^{-2} N m^{-2}).

(110°W), where the southerly wind stress is one-half of that on the coast. The SST anomaly at $x = x_E$ increases with coupling strength in a nonlinear manner, slowly at low coupling and rapidly at high coupling (Fig. 12a). Outside the southerly forcing region (west of 110°W), SST anomalies decay westward exponentially (Fig. 10). The *e*-folding length scale for the westward decay of SST anomaly increases as coupling strengthens (Fig. 12b) in a qualitative agreement with the theory.

It is interesting to consider a case where the external easterly is removed ($\overline{U} = 0$). We let $T_c = T_0$ because the SST in the surrounding oceans reaches this equilibrium temperature in the absence of easterly induced upwelling. With a flat thermocline in the basic state, the southerly winds are the only cause of zonal asymmetry. Figure 13 depicts the development of zonal asymmetry in the intermediate model as the coupling strengthens. The southerly induced upwelling initiates a cooling in SST in the east, which is amplified and spread out westward by the Bjerknes feedback. As a result, easterly winds and a tilt of thermocline are established. Compared with Fig. 6a, however, the cold tongue is much too weak without extra easterly forcing.

5. Discussion

The Pacific ocean–atmosphere system displays pronounced asymmetries in both the zonal and meridional directions. Based on experiments with an intermediate coupled model, this study shows that the latitudinal asymmetry exerts a great impact on the development of the Walker circulation and equatorial cold tongue. In an ocean model simulation forced by observed winds, the southerly cross-equatorial winds associated with the NH ITCZ is imperative for cooling the far eastern Pacific where equatorial upwelling vanishes because zonal winds are blocked by the Andes. These southerly winds affect sea surface temperature by inducing upwelling along the South American coast and in the open ocean

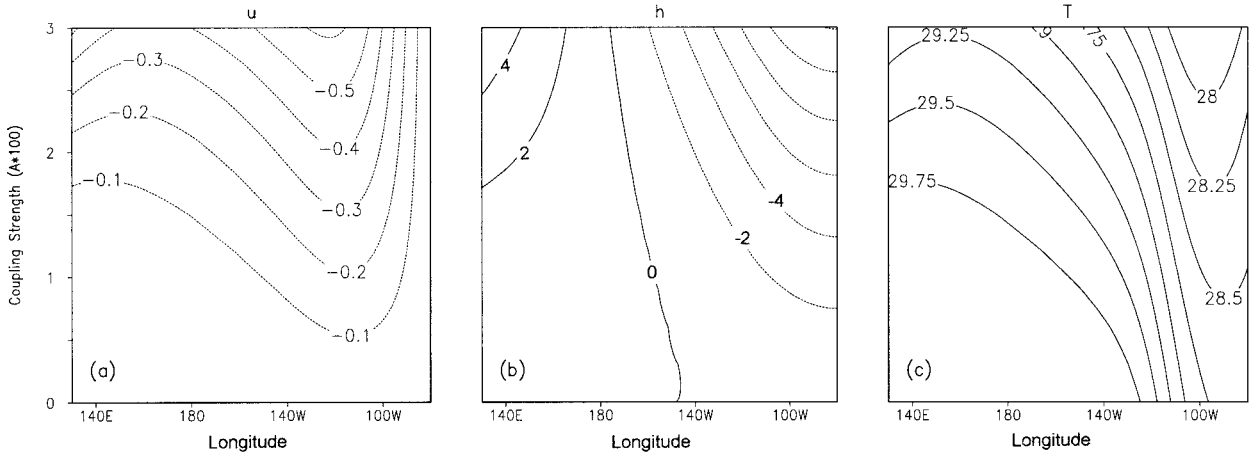

FIG. 13. Zonal distributions of (a) zonal wind stress (10^{-2} N m^{-2}), (b) thermocline depth, and (c) sea surface temperature as functions of coupling coefficient in model runs with the external easterly wind removed.

to the south of the equator. The equatorial annual cycle in SST is cited as observational evidence in support of the proposed mechanism that the southerly winds control the strength of the equatorial cold tongue.

Although strong cross-equatorial winds are observed only in the eastern Pacific, the effect of these southerlies in the coupled system is not limited to the east but reaches the whole ocean domain. This happens because of the Bjerknes feedback between the SST gradient and zonal wind. The cooling caused by southerlies in the east increases the SST contrast with the west, inducing easterly wind anomalies across the Pacific. Enhanced easterlies raise the thermocline in the east and strengthen upwelling, both leading to a further cooling in the central and eastern Pacific. In this sense, a substantial portion of the easterly winds at the equator can be attributed to the southerly wind forcing as part of the coupled response (the difference between the $\tau_y \neq 0$ and $\tau_y = 0$ M curves in Fig. 8). A simple analog model is derived, which extends previous point-coupling models (Neelin and Dijkstra 1995) by explicitly including the zonal dimension. This analog model reveals two separate roles played by the Bjerknes feedback: it amplifies the cooling by the southerly wind forcing in the eastern ocean, and at the same time, it spreads the cooling to regions that are free of southerly winds. The enhancement of easterly winds is central to both roles of the Bjerknes feedback.

However, the same intermediate model does not produce a realistic cold tongue under a conventional setting with the southerly forcing removed. Instead of intensifying the cooling induced by the external easterly wind, the Bjerknes feedback acts to move the SST minimum to the west. This happens because the contrast between the warm South America and the cold eastern ocean generates westerly wind anomalies, leading to an increase in SST in the east. As a result, only a weak cold tongue is possible, with the largest cooling found in the central part of the basin.

The development of the Walker circulation–cold tongue complex is forced by forcings external to the equatorial ocean–atmosphere system. One of these external forcings is the modest easterly wind maintained by the global Hadley circulation and eddy-momentum transport. This study proposes an additional, complementary forcing mechanism—the southerly cross-equatorial wind in the eastern Pacific. Each of these forcings can break the zonal symmetry, but only their combined effect gives rise to a cold tongue that is realistic in both intensity and zonal structure (Fig. 14). This suggests that both forcings are essential to the formation of the Walker circulation–cold tongue complex. In particular, the southerly forcing anchors the SST minimum to the eastern Pacific. If the earth's climate were symmetric about the equator, the meridional wind would vanish along the equator. There would still be a cold tongue under the zonal mean easterly forcing, but it would be much weaker and have a different zonal structure than what we see today. This hypothesis can be easily tested by contrasting coupled GCM runs under realistic and latitudinally symmetric settings.

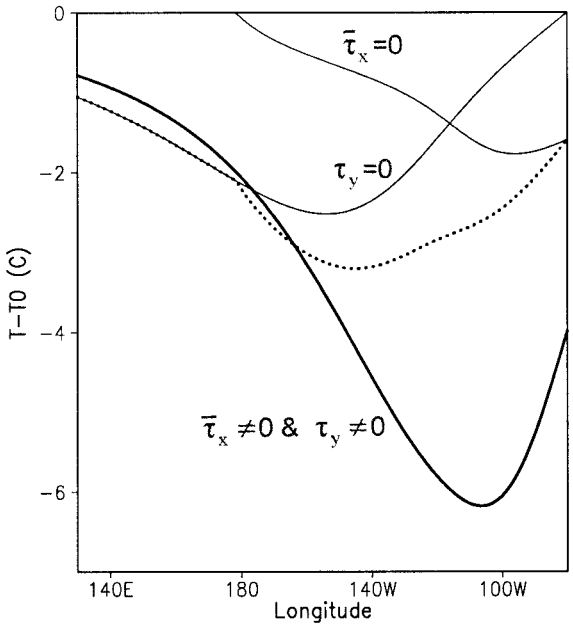

FIG. 14. Sea surface temperature departure from its equilibrium value as a function of longitude ($A = 0.025$ N m^{-2}). The mountain blocking is included and $T_c = 29$°C in all three sets of runs. Notice that the cold tongue forced by either external easterly or southerly wind only is quite weak. The sum (dotted line) of the response to each forcing is much smaller than the response to the combined forcing.

Acknowledgments. The author thanks Atsushi Kubokawa and Tony Hirst for helpful discussions and Ed Schneider for comments on an earlier version of the manuscript. This work is supported by grants from the Japanese Ministry of Education and the Center for Climate System Research of the University of Tokyo.

REFERENCES

Battisti, D. S., and A. C. Hirst, 1989: Interannual variability in a tropical atmosphere–ocean model: Influence of the basic state, ocean geometry, and nonlinearity. *J. Atmos. Sci.,* **46,** 1687–1712.

Bjerknes, J., 1969: Atmospheric teleconnections from the equatorial Pacific. *Mon. Wea. Rev.,* **97,** 163–172.

Cane, M. A., M. Munnich, and S. E. Zebiak, 1990: A study of self-excited oscillations of the tropical ocean–atmosphere system. Part I: Linear analysis. *J. Atmos. Sci.,* **47,** 1562–1577.

Dijkstra, H. A., and J. D. Neelin, 1995: Ocean–atmosphere interaction and the tropical climatology. Part II: Why the Pacific cold tongue is in the east. *J. Climate,* **8,** 1343–1359.

Gill, A. E., 1980: Some simple solutions for heat-induced tropical circulation. *Quart. J. Roy. Meteor. Soc.,* **106,** 447–462.

Hao, Z. J., J. D. Neelin, and F. F. Jin, 1993: Nonlinear tropical air–sea interaction in the fast wave limit. *J. Climate,* **6,** 1523–1544.

Hirst, A. C., 1986: Unstable and damped equatorial modes in simple coupled ocean–atmosphere models. *J. Atmos. Sci.,* **43,** 606–630.

Huang, B., and E. K. Schneider, 1995: The response of an ocean general circulation model to surface wind stress produced by an atmospheric general circulation model. *Mon. Wea. Rev.,* **123,** 3059–3085.

Jin, F. F., and J. D. Neelin, 1993: Modes of interannual tropical ocean–atmosphere interaction—A unified view. Part I: Numerical results. *J. Atmos. Sci.,* **50,** 3477–3503.

Kleeman, R., 1989: A modelling study of the effect of the Andes on the summertime circulation of tropical South America. *J. Atmos. Sci.,* **46,** 3344–3362.

Lindzen, R. S., and S. Nigam, 1987: On the role of sea surface temperature gradients in forcing low level winds and convergence in the tropics. *J. Atmos. Sci.,* **44,** 2418–2436.

Liu, Z., and B. Huang, 1997: A coupled theory of tropical climatology: Warm pool, cold tongue, and Walker circulation. *J. Climate,* **10,** 1662–1679.

Ma, C.-C., C. R. Mechoso, A. W. Robertson, and A. Arakawa, 1996: Peruvian status clouds and the tropical Pacific circulation—A coupled ocean–atmosphere GCM study. *J. Climate,* **9,** 1635–1645.

Matsuno, T., 1966: Quasi-geostropic motions in the equatorial area. *J. Meteor. Soc. Japan,* **44,** 25–43.

Mitchell, T. P., and J. M. Wallace, 1992: The annual cycle in equatorial convection and sea surface temperature. *J. Climate,* **5,** 1140–1156.

Neelin, J. D., 1991: The slow sea surface temperature mode and the fast-wave limit: Analytical theory for tropical interannual oscillations and experiments in a hybrid coupled model. *J. Atmos. Sci.,* **48,** 584–606.

——, and H. A. Dijkstra, 1995: Ocean–atmosphere and the tropical climatology. Part I: The dangers of flux correction. *J. Climate,* **8,** 1325–1342.

Numaguti, A., and Y.-Y. Hayashi, 1991: Behavior of cumulus activity and the structures of circulations in an ''aqua-planet'' model. Part II: Eastward-moving planetary scale structure and the intertropical convergence zone. *J. Meteor. Soc. Japan,* **69,** 563–579.

Philander, S. G. H., and R. C. Pacanowski, 1981: The oceanic response to cross-equatorial winds (with application to coastal upwelling in low latitudes). *Tellus,* **46,** 201–210.

——, D. Gu, G. Lambert, T. Li, N.-C. Lau, and D. Halpern, 1995: Why the ITCZ is mostly north of the equator. *J. Climate,* **9,** 2958–2972.

Suarez, M. J., and P. Schopf, 1988: A delayed action oscillator for ENSO. *J. Atmos. Sci.,* **45,** 3283–3287.

Woodruff, S. D., R. J. Slutz, R. L. Jenne, and P. M. Steurer, 1987: A comprehensive ocean–atmosphere dataset. *Bull. Amer. Meteor. Soc.,* **68,** 521–527.

Xie, S.-P., 1994: On the genesis of the equatorial annual cycle. *J. Climate,* **7,** 2008–2013.

——, 1996: Westward propagation of latitudinal asymmetry in a coupled ocean–atmosphere model. *J. Atmos. Sci.,* **51,** 3236–3250.

——, and S. G. H. Philander, 1994: A coupled ocean–atmosphere model of relevance to the ITCZ in the eastern Pacific. *Tellus,* **46A,** 340–350.

Zebiak, S. E., and M. A. Cane, 1987: A model El Niño–Southern Oscillation. *Mon. Wea. Rev.,* **115,** 2262–2278.